Diyala Journal of Engineering Sciences

Journal homepage: https://djes.info/index.php/djes

ISSN: 1999-8716 (Print); 2616-6909 (Online)

Designing Efficient Hybrid Photovoltaic and Battery Energy Storage Systems with Optimal Controlling and Management

Ali M. Al-Jumaili[1*], Mohammed Sami Mohammed[2], Manal T. Ali[1] and Adham Hadi Saleh[1]

[1] Department of Electronics Engineering, University of Diyala, 32001 Diyala, Iraq
[2] Department of Pure Science-Computer, University of Diyala, 32001 Diyala, Iraq

ARTICLE INFO

Article history:
Received: 27/03/2025.
Revised: 19/01/2026,
Accepted: 23/02/2026.
Available online: 15/06/2026.
Keywords:
Improved Grey Wolf Optimization
Maximum Power Point tracking
Photovoltaic
Voltage regulation
Energy storage

ABSTRACT

A novel control strategy was introduced for enhancing the performance of photovoltaic (PV) systems integrated into the power grid. The proposed method applied an Improved Grey Wolf Optimizer (IGWO) directly for Maximum Power Point Tracking (MPPT) in PV systems. The main goal is to maximize the output power extracted from the PV panels under varying environmental conditions while in the same stage improving the power quality delivered to the grid through keeping the stable voltage and frequency at the same required levels. A detailed simulation model was obtained using MATLAB/Simulink, including the PV array, DC-DC boost converter, and grid-connected inverter. The IGWO algorithm was employed to determine the optimal controlling signals for MPPT, that providing in high dynamic performance compared to traditional techniques. Simulation was included list of three cases in solar irradiance and load variations to evaluate the effectiveness of the controller. The proposed IGWO-based MPPT strategy achieved higher output power from the PV system compared to the selected traditional method as P&O. In addition, the method effectively minimized the Total Harmonic Distortion (THD) and ensures voltage with frequency stability at the point of common coupling. The designing of a single optimization control for the PV framework based on IGWO technique was the main novelty of this work through the integration between the regulated grid voltage and frequency stabilization. This control strategy enhanced the reliability, making it a strong candidate for next-generation renewable energy integration.

1. INTRODUCTION

Hybrid photovoltaic (PV) systems integrated with Battery Energy Storage Systems (BESS) have emerged as a one solution for achieving stable with reliable, and clean energy in both grid and off grid connected environments. These systems include PV panels, BESS, and sometimes auxiliary sources such as mentioned for the wind turbines and the diesel generators in [1,2]. For this reason and to achieve this configuration, maintaining power quality, ensuring system stability, and improving efficiency require intelligent energy management and optimization strategies. Different types of control strategies have been proposed in literature for energy management, including adaptive Neuro-Fuzzy Inference Systems (ANFIS) for Maximum Power Point Tracking (MPPT) as suggested in [3], or the suggestion study by authors in [2] using per-phase dq control for grid-forming BESS, and droop control techniques for DC bus voltage regulation as studied in [4]. The State of Charge related to a battery is managing by using the Power Management Systems (PMS) and affected by several inputs such as load conditions as presented and determined in [5]. The system stability and the overall cost for the BESS could be highly achieved through optimizing the component sizing. Several studies have been introduced to optimize this parameter as in the using of the Gravitational Search Algorithm (GSA) and Mixed-Integer Linear Programming (MILP) which suggested by authors in [6] and [7]. These techniques have been also applied for power flow balancing in hybrid systems not only for the size adjusting. However, these studies overlook dynamic operational constraints, particularly in MPPT control under fluctuating weather or partial shading, and real-time power exchange with the grid. A major research gap remains in simultaneously addressing as undefined real-time MPPT under dynamic conditions using intelligent bio-inspired algorithms. Also, the optimal power flow and inverter voltage control to supply active power to the grid. In addition, grid

* Corresponding author's E-mail: ali.mh@uodiyala.edu.iq
DOI: 10.24237/djes.2026.19210

frequency/voltage regulation under variable load scenarios using a unified framework. This study studied and detailed the above gap by proposing an enhanced bio-inspired Grey Wolf Optimizer (IGWO) for MPPT, integrated with a grid-connected PV inverter system which able to manage the real-time energy and grid functions. Recent studies confirm the effectiveness of utilizing IGWO in dynamic solar environments, particularly in handling partial shading and improving MPPT response time as mentioned in [8].

In previous research, several MPPT and control methods have been introduced. Conventional MPPT algorithms like Perturb and Observe (P&O) are simple but suffer from steady-state oscillations under fast-changing irradiance as mentioned in [9]. Advanced algorithms like Grasshopper Optimization Algorithm (GOA) and Particle Swarm Optimization (PSO) offer better adaptability as mentioned in [10], while Incremental Conductance (IC) shows high accuracy under varying weather conditions [11]. However, these methods often less effective when high performance is needed under extreme fluctuations or high loads [12,13]. Artificial intelligence techniques, including neural networks and fuzzy logic controllers, showed promise in improving MPPT performance as suggested in [14,15]. Also, dual-axis tracking and converter-level optimization improve power extraction in shaded conditions was presented in [13,16]. A few studies consider integrated optimization of MPPT, inverter control, and power exchange with the grid, especially using bio-inspired approaches. Recent research has shown that multi-level hybrid energy systems, when optimized using nature-inspired algorithms enhanced power quality and system responsiveness in smart inverter designs as mentioned in [17].

Authors in [18] implemented a high-efficiency LLC resonant converter system for a 3 kW PV array, enhancing converter-level energy transfer efficiency. Also, authors in [19] demonstrated evolutionary optimization of resonant converters for improved energy management. Techniques based on artificial intelligence, like artificial neural networks and fuzzy logic controllers, have demonstrated promise in enhancing voltage regulation and MPPT performance as explained in [19, 20]. In order to optimize energy harvesting and use in PV systems, the field is still focused on creating methods that can deal with partial shading circumstances, quick environmental changes, and overall system optimization. The study described in this article is based on a large body of prior research that investigates energy management control and optimization in hybrid autonomous PV systems, especially those that are coupled with BESS. The work of [21], who created a high-efficiency LLC resonant converter system for a 3 kW PV solar array, provided a solid basis for this investigation. In order to design power converters that were essential to effective energy conversion and management in photovoltaic systems, this work demonstrated the use of finite automated systems. In order to maximize energy efficiency and minimize losses, the converter is essential for regulating the energy flow between the solar panels, the energy storage system, and the load. In [22], work on evolutionary design automation for series resonant converters in solar systems was another important study that expanded the field of power electronics. In order to enhance total system efficiency, their study concentrated on improving the design of power converters that enabled the integration of PV arrays with energy storage devices. In order to improve the efficiency of power conversion even in dynamic and variable operating situations, their method makes use of evolutionary algorithms to improve the performance of series resonant converters. Since they emphasize the significance of intelligent converter design in preserving high energy efficiency and stable system operation, the study's conclusions were extremely pertinent to the optimization of hybrid PV systems with battery energy storage.

The optimization of PV array dimensions under shading conditions, as shown in [16], further highlights the need for holistic system-level design. Recent studies as well focused on the control mechanism as in [23], when authors introduced an innovative mode-selective control approach for optimally charging Li-ion batteries in PV systems based on real-time solar irradiation and battery SOC. The combination of the buck converter and gain control was the main techniques suggested in the previous article. This work was introduced to improve charging efficiency in addition to minimize the power loss and battery stress.

The integrating process between the BESS within PV system using the optimization characteristics of IGWO to trace the accurate MPPT was the main purpose of this study. These suggestions were also done for rapid irradiance variation with some mentioned conditions. This was not the only objective for this study but also the enabling of voltage regulation with active power delivery as well. Moreover, keeping the grid of PV system stability based on these different conditions. The overall system that related to selected PV is to design a hybrid system of BESS managed through IGWO to enhance the reliability and stability. Also, an IGWO was applied for real-time MPPT, and compared to the traditional techniques under the same taken conditions for both techniques to demonstrate the results. Moreover, the handling real time changing loads is also the purpose of this design to keep the optimal voltage and provides accurate power to the grid. The results that will be obtained to demonstrate the benefits of the proposed optimization technique with voltage stability, and reduced power losses. The paper structure is set out as follows: The suggested system structure is described in Section 2, the simulation results and

discussion are shown in Section 3 and the study is concluded in Section 4.

2. METHODS AND MATERIALS

2.1 Proposed system configuration

A solar PV array, lithium-ion batteries, a DC/DC converter, a bidirectional DC/AC inverter, a power transformer, multiple loads, a utility grid, and an energy management and control unit make up the overall structure of the suggested system, as shown in Figure 1. In order to regulate the DC voltage, grid voltage, and frequency under various operating situations, the energy management and control unit creates the best control signals for each component based on real-time data from the grid, PV array, and battery.

In this proposed system, the DC-DC converter is responsible for regulating the DC voltage levels obtaining from the PV array and the battery, ensuring they are suitable for feeding the DC-AC inverter or supplying the load. The controller adjusts the duty cycle of the DC-DC converter to ensure the DC voltage remains within the required range, effected dynamically to changes in load or generation. The control equation for the PI controller is given in equation below:

$$V_{DC} = K_P \cdot (V_{set} - V_{measured}) + K_i \cdot \int (V_{set} - V_{measured}).dt \quad (1)$$

Where V_{DC} is the controlled DC voltage, V_{set} is the reference DC voltage, $V_{measured}$ is the measured DC voltage, K_p and K_i are the proportional/integral gains, respectively.

The related power given in equ.2 and equ.3 are the main two parts of the inverter output power, that will be utilized to regulate the DC-AC inverter's output current. These components are the active power (P_p) and reactive power (Q_q), which controlled using the d_q control approach based on the d-axis and q-axis in the rotating reference frame. These two parts are given in the equations below:

$$P_p = V_d \cdot I_d + V_q \cdot I_q \quad (2)$$

$$Q_q = -V_d \cdot I_d + V_q \cdot I_q \quad (3)$$

Where the P_p and the Q_q are the active and reactive inverter powers respectively. In the other hand the V_d and V_q are the d-axis and q-axis voltages, while the I_d and I_q are the d-axis/q-axis currents.

The EMS adjusts the inverter's duty cycle to ensure that the voltage and frequency are synchronized with the grid, guaranteeing efficient energy transfer with minimizing harmonic distortion.

Using a bio-inspired MPPT optimization approach, the solar panels' efficiency is increased. The Flower Pollination Algorithm (FPA) and IGWO are used in this study to maximize the PV array's output power. While the grid connection is accomplished by the d_q control approach, which synchronizes the bidirectional inverter with the grid and the DC source, the battery uses a PI control mechanism to guarantee the stability of the DC bus voltage.

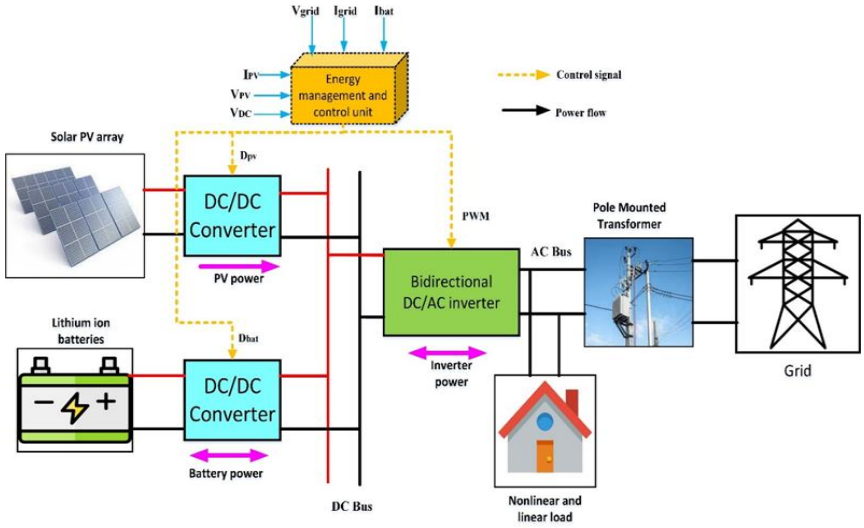

Figure 1. Proposed hybrid PV/battery system for ON-grid application

2.2 Modelling of the PV system

A few advantages of the single-diode model of a solar cell, as shown in Figure 2, include its simplicity, ease of efficiency analysis, parameter extraction, design optimization, and applicability for basic research as well as instructional and computational applications [24]. The activity of the solar cell is represented in this model in a straightforward but useful way, which facilitates analysis and understanding. In addition, this will make the process more easy to optimize the performances of each cell in the overall solar panel. Also, the requirements of rapid simulations make the use of one diode are appropriate. Moreover, it will be useful for the parameter extraction, design optimization, and preliminary as suggested in [25]. The following is an expression for the solar cell's output current: solar cell can be written as follows:

$$I = I_{ph} - I_o \left(\exp\left[\frac{(V+IR_S)}{aA}\right] - 1 \right) - \frac{(V+IR_S)}{R_{sh}} \quad (4)$$

$$I_o = \frac{I_{SC} + K_I(T - T_n)}{exp\left(\frac{q(V_{OC} + K_V(T - T_n))}{a\ K\ N_S T}\right) - 1} \quad (5)$$

$$I_{ph} = (I_{SC} - K_I\ (T - T_n))\frac{G}{G_n} \quad (6)$$

The electrical behavior of the PV module is defined by a number of several parameters such as the module voltage, that refer to the potential difference across the module. Also, the module current, that refer to the output current of solar cell. The current produced by the PV module as the photocurrent (I_{ph}), and the current is also known as the diode's saturation current (I_o). The losses as another parameter are taken into consideration referring to R_S and R_{sh} respectively. The R_{sh} refers to the leakage current across the module, while the RS refers to the internal resistance of the module. Furthermore, the overall efficiency of the equivalent circuit will be referred to as (a) symbol. Additionally, the open-circuit voltage is denoted as (V_{OC}), which refers to the voltage across the module that has no load situation. While, the short-circuit current denoted as the (I_{SC}) and refers to the current in shorted case. The working PV module characteristics have been given through these parameters under some circumstances. The performance of PV module is affected by temperature of the surrounding environment, that denoted as (T). the standard testing conditions as denoted STC, specifying the temperature as Tn which is normally 25°C will be used as a reference. The way of module behavior based on the temperature changing is important to understand the module performances. This will be done through the specified voltage and current coefficient that denoted as (K_V) and (K_I) respectively. These operations are also depends on other physical parameters, like the Boltzmann constant (K) and the thermal voltage (A). in addition to the electron charge (q) is also a crucial parameter for determining current and voltage at the device level. Finally, the module's output power is determined by the number of cells (Ns). The combinations of thee parameters are allowing for performance optimization across a range of operating and environmental circumstances.

2.3 The type of Lithium-ion battery

The type of these batteries is a popular choice for such an application and also recommended for energy storage in PV system due to many benefits as presented in [26]. High efficiency, quick charging and discharging, and a low self-discharge rate are some of these benefits. Lithium-ion batteries are a perfect option for solar energy storage because of their high energy density, extended cycle life, scalability, and general dependability. In solar power systems, their capacity to store and effectively manage energy guarantees peak performance and utilization.

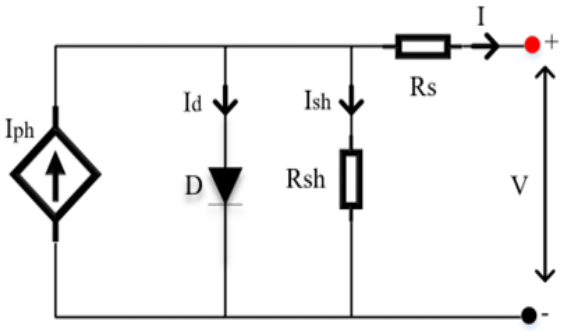

Figure 2. Solar cell circuit using single diode based on the proposed model

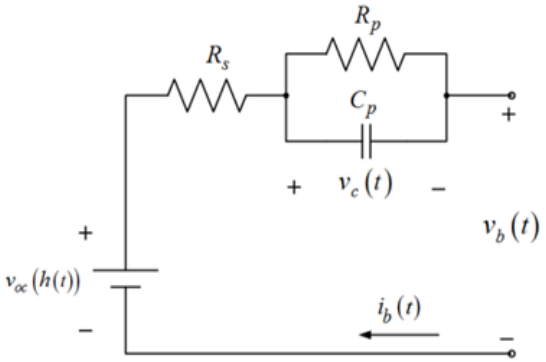

Figure 3. Electrical circuit of a battery

The battery's electrical circuit is depicted in Figure 3. However, as illustrated in Figure 3, temperature and SOC have an impact on the battery's equivalent circuit parameters, including series resistance (Rs), parallel resistance (R_p), and capacitance (C_p) [27, 28]. For the course of the observation period, S_{OC} and temperature can be regarded as time-invariant because of their comparatively tiny time variations. Consequently, the temperature and S_{OC} variations are so small that they can be considered constant during the identification procedure, with a certain amount of uncertainty. This allows for the rapid, real-time identification of these parameters without being greatly impacted by slight variations in temperature or S_{OC}. The battery's behavior is represented mathematically below [27, 28], where $V_c(t)$ denotes the voltage stress on the circuit and $V_b(t)$ and $i_b(t)$ denote the battery's output voltage and current, respectively.

$$v_b(t) = v_{oc}\big(h(t)\big) - R_s\ i_b(t) - \ v_c(t) \quad (7)$$

$$\frac{dv_c(t)}{dt} = -\frac{1}{C_b\ R_b} v_c(t) + \frac{1}{C_b}\ i_b(t) \quad (8)$$

2.4 Proposed EMS system

Enhanced energy efficiency, smooth integration of renewable energy sources, cost savings, and better demand response and load management are just a few advantages of combining a DC/AC microgrid (MG) with an Energy Management System (EMS). One of the main benefits of MGs is their autonomy, which reduces grid congestion and the likelihood of blackouts while guaranteeing a dependable power supply to vital loads. The suggested system's EMS and control framework are

shown in Figure 4. Battery management, MPPT optimization, and grid-connected inverter control are its three primary control methodologies. By modifying the duty cycles of the inverter switches or circuits, boost converter, and bidirectional converter, the suggested EMS efficiently manages energy flow and maximizes system efficiency. The evaluation process was also done to calculate the Total Harmonic Distortion (THD), which is helpful to show how the power is clean and stable in the proposed PV–BESS. The THD was given in equation (9) which mentioned as in [29].

$$\mathrm{THD_I} = \frac{\sqrt{\sum_n^H I_n^2}}{I_{fund}} \quad (9)$$

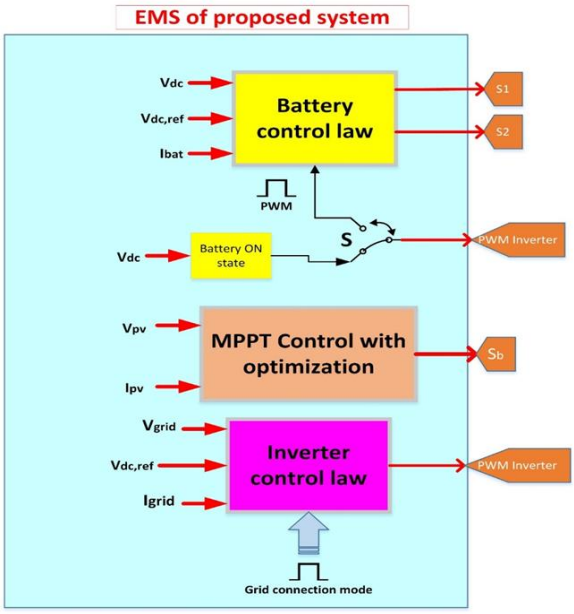

Figure 4. The suggested EMS and control scheme

The suggested Baseline rule-based Energy Management System (EMS) flowchart for the DC/AC microgrid (MG) system is shown in Figure 5. This flowchart shows the exact steps that the EMS takes to guarantee effective energy utilization and maximize microgrid performance. The EMS is in charge of monitoring the battery and grid-connected inverter as mentioned before. It starts by checking the important parameters and metrics as load demand and battery SOC. In order to optimize efficiency, the EMS uses this data to calculate the ideal energy flow between the battery, solar panels, and the grid. The flowchart as shown in Figure 5, firstly are related to the battery management. The Ems responsible of the determination of the charging period and discharging period as well for the battery, and for keeping it working as optimal as possible with ideal power delivery to the load. Some parameters will have decided the charging and discharging time like the current in SOC case and power requirement. Based on the extracted power from the PV panel, the EMS optimize it using MPPT and ensures the solar system runs efficiently by modifying the PV module operation point. Advanced optimization methods, like bio-inspired algorithms, which dynamically modify the system's parameters for optimal power extraction, form the foundation of the MPPT control rule. The last step of the flowchart in Figure 5 is the control of the grid-connected inverter and done through modifying the duty cycle of the inverter switches. The EMS ensures the inverter runs in unison with the grid to guarantees that the microgrid draw power from the grid when necessary. Based on the duty cycle value, the EMS will optimize the related PV parameters during the whole process. This last step demonstrates the efficiency of system and balanced in the face of variations in energy consumption. The charging and discharging power are considering as a controlling parameter within the IGWO design which is limited by SOC constraints. optimized battery power reference is generated at each control interval to support load balancing, and reduce grid dependency. The battery control law then enforces these optimized set points in real time, ensuring safe and coordinated operation under both normal and grid-disconnected scenarios. While Figure 6, showed that at each control time step, the EMS receives real-time measurements of the PV generation, and the BESS-SOC. These inputs will be processed by the EMS and forwarded to the IGWO, which determines the optimal power sharing among the overall system by minimizing a defined function subject to operational constraints. Based on the optimized power references provided by IGWO, the EMS will select the appropriate operating mode, include the charging and discharging regarding the SOC limits. The BESS SOC is then updated, and the process will be repeated at the next step, enabling adaptive management under varying operating cases.

2.5 Optimization based MPPT Control

In solar systems, traditional techniques related to monitoring MPPT usually depend on a number of algorithms intended to maximize the power production from PV panels as presented in [30, 31]. These traditional techniques worked poorly, especially when load is changing continuously and so fast that cause higher oscillations and slower adjustments as mentioned in [32, 33]. Advanced techniques related to the observing the MPPT provide solar systems with a number of significant benefits like fault tolerance increasing, faster reaction times, better performance in dynamic environments, and improved capabilities for accurate monitoring within data analysis. Additionally, these techniques assist in the advancement of solar technology research as suggested in [34]. The using of such techniques increases the efficiency and dependability of solar systems, advancing the development of solar energy technologies. One of the basic methods to optimize MPPT and offering a reliable way to monitor the PV system power. The same characteristics of the machine learning introduced by

the IGWO by providing dynamic tracking under real-time conditions. There are four types of classifications in the grey wolves' main process as α, β, δ, and ω wolves and each role is different in the optimization process.

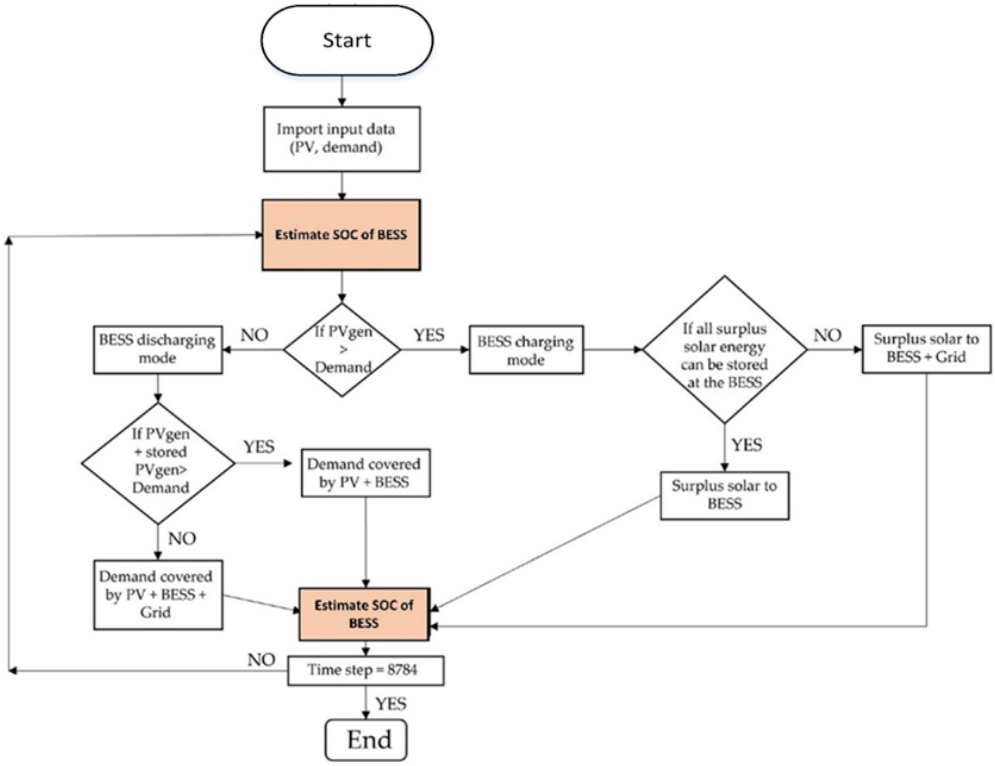

Figure 5. Baseline rule-based Energy Management System (EMS) flowchart for the DC/AC microgrid (MG)

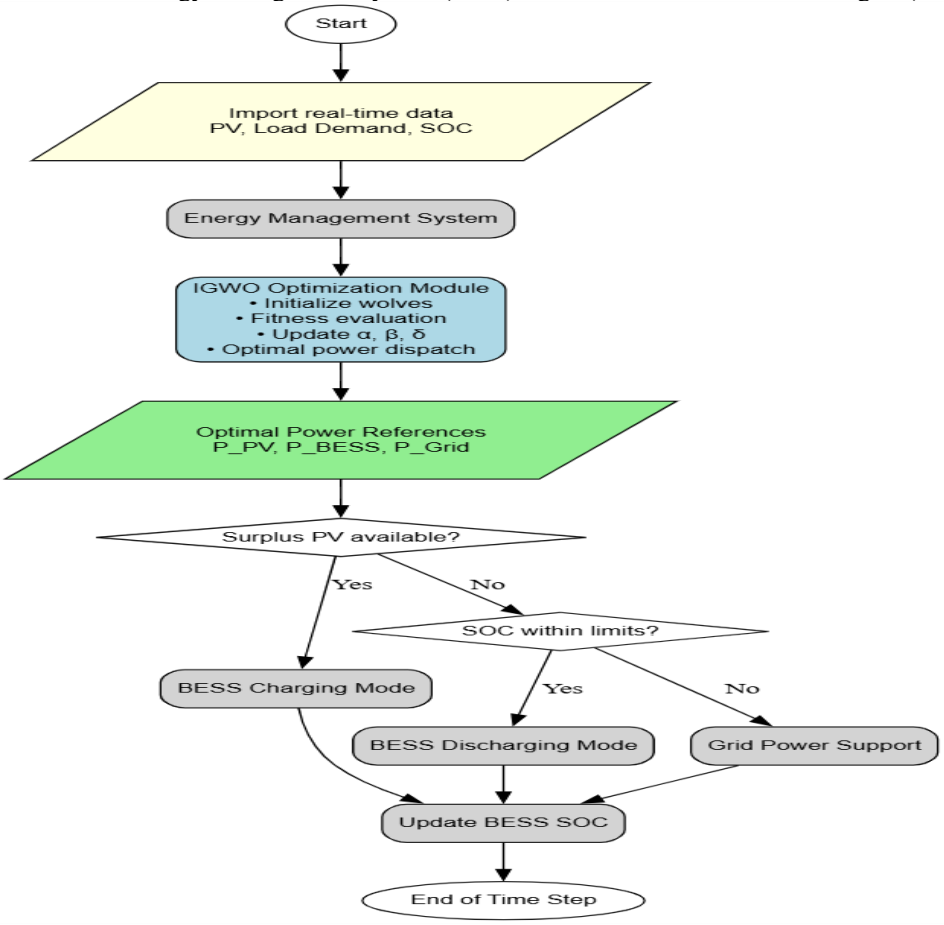

Figure 6. IGWO-based optimal energy management framework

The leading of the optimization process was based on alpha with the other wolves following in unison to find the best solution. The optimization technique based on this technique is shown in Figure 7, which showed the

process of finding the best solutions. The equations from (10) to (14) as described in [33, 34] that responsible for all wolf's movement and update the overall process. The efficiency of PV system is enhanced through using these equations, that making the searching process of maximum points available. The traditional techniques of optimizing the MMPT as presented by authors in [35], which introduced for shading parameter only. This study introduces an enhanced IGWO-based MPPT controller designed for maximizing the PV power obtained in different cases and also regulate grid voltage and frequency. The integration of EMS, IGWO, and dq-synchronized inverter control into a single structure represents a novel contribution, particularly in improving power quality in grid-connected PV systems.

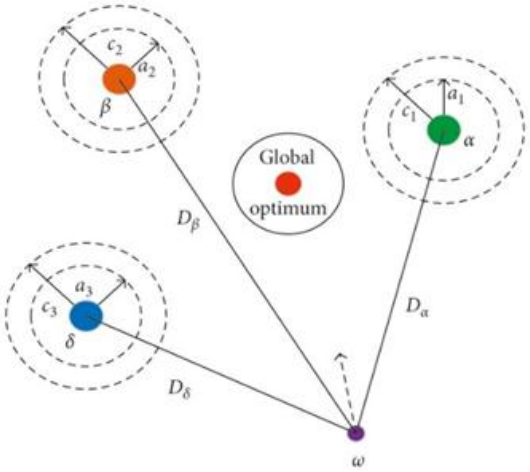

Figure 7. Conceptual representation of IGWO

$$D_\alpha = |C_1.X_\alpha(t) - X(t)|$$
$$D_\beta = |C_2.X_\beta(t) - X(t)| \quad (10)$$
$$D_\delta = |C_3.X_\delta(t) - X(t)|$$

$$X_1(t+1) = X_\alpha(t) - A_1.D_\alpha$$
$$X_2(t+1) = X_\beta(t) - A_2.D_\beta \quad (11)$$
$$X_3(t+1) = X_\delta(t) - A_3.D_\delta$$

$$X(t+1) = \frac{X_1(t+1) + X_2(t+1) + X_3(t+1)}{3} \quad (12)$$

where X(t) is the current location of teach wolf individual separately. While, the $X_\alpha(t)$, $X_\beta(t)$ and $X_\delta(t)$ are the positions of the related wolves, respectively. In the other hand, the random coefficients are denoted as A and C as given in equation (13) and equation (14).

$$A = a(2\,r_1 - 1) \quad (13)$$
$$C = 2r_2 \quad (14)$$

An enhanced MPPT technique based on the IGWO is presented in this study to improve grid-connected inverter power quality and photovoltaic (PV) system performance. The following succinctly describes the main goals of utilizing this IGWO-based MPPT:

- The IGWO-based MPPT algorithm increases the overall efficiency of PV system due to the accurate monitoring of MMPT. This will also lead to enhance energy conversion that provided optimal performances by the system.
- The IGWO algorithm has quick convergence and precise MPPT optimization and working with better results than traditional techniques in dynamic situation.
- The IGWO-based MPPT's capacity to adjust to different cases by ensuring that the system has a stable run at its MPP.

The program that has been utilized for this work was the MATLAB based on these lists:

1- The random initialization of wolves will be the first step that each wolf will represent a possible solution. The overall parameters have been mentioned to determine the PV operating points.
2- The level of each individual wolf will be determined based on the objective function and mathematical model.
3- The highest fitness and wolf level will be determined based on α, β, and δ regarding their performances of PV system. The rest wolves position will be determined based on the first wolves to calculate the cost function.
4- The boundary management strategies will be utilized to keep the recently wolf in its locations based on the specified range.
5- Reevaluate the new positions' level of fitness and adjust the wolves' fitness values appropriately.

Continue stages three through six until a termination condition is satisfied, like completing a certain number of iterations or performing to a satisfactory level. Figure 8 displays the flowchart of the Improved IGWO algorithm, which graphically depicts these processes. This study primarily focuses on simulation-based validation using MATLAB/Simulink, which do not capture all real-world uncertainties such as hardware losses, and communication delays. Moreover, the performance of the IGWO-based MPPT controller has not been tested under all climatic variations, particularly extreme weather conditions. Future work will involve hardware-in-the-loop testing and extended case studies across different geographical regions to assess real-time applicability and robustness. This work introduces several key innovations that differentiate it from existing related works by some points. In this paper using an enhanced version of IGWO that incorporates adaptive learning strategies and speed of tracking in real-time compared to traditional methods. Also, the simultaneous optimization of the PV system's power extraction and the management of the grid-connected inverter, which ensures that the system operates with reducing harmonic distortion and optimizing the transfer of excess power to the grid. Previous works have not fully integrated IGWO-based MPPT control with grid frequency and voltage regulation as mentioned in the previous paragraphs. In addition to IGWO, bio-inspired algorithms employment the FPA

and IGWO to maximize PV array output, providing a hybridized MPPT strategy that offers improved energy harvesting efficiency. This is a step forward from relying on a single algorithm to ensure maximum utilization of PV resources, particularly in non-ideal weather conditions. Also, the EMS in this design uses real-time data to adjust the duty cycles of the bidirectional inverter and other converters based on the IGWO's optimized power point, which improves system response to rapid load. This level of real-time optimization is less common in existing literature where simpler MPPT algorithms often didn't success to adjust quickly in the face of unpredictable conditions. By integrating these features, this paper offers more reliable, flexible approach to PV-battery systems, particularly in grid-connected scenarios.

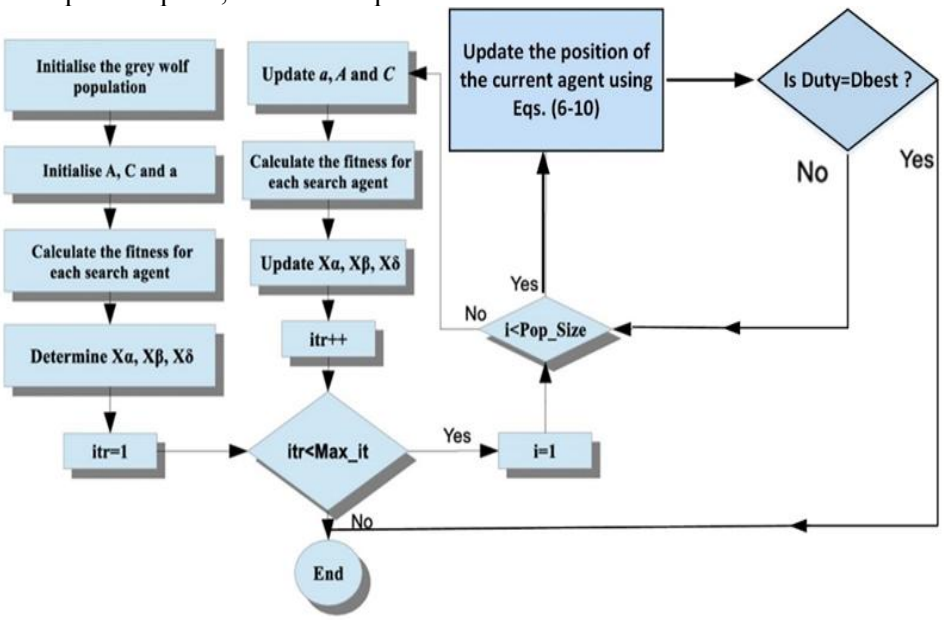

Figure 8. Flowchart of IGWO

3. SIMULATION RESULTS AND DISCUSSION

3.1 Optimization parameters of related IGWO

In order to explore and take advantage of the search space, IGWO mimics the interactions between alpha, beta, delta, and omega wolves. For the purpose of finding the best answer in a search space, these wolves iteratively change their places. The population size, or the number of potential wolves in each iteration, was 20. Since the population size in this instance is set at 20, there were 20 possible wolves searching the area. More possible solutions were taken into consideration as the population grew, which may improve exploration but may also raise computing costs. For many situations, a population size of 20 provided a balance between processing expense and exploration. The optimization method updated the wolves' positions up to 200 times or until the stopping requirements were satisfied, with a maximum of 200 iterations. Based on their interactions with the alpha, beta, and delta wolves, the wolves got closer to the ideal solution with each iteration. The method was prevented from running endlessly by the maximum number of iterations. Nevertheless, based on the algorithm's pace of convergence, the ideal solution was discovered before 200 iterations. Every wolf location was represented by a vector, each of which elements were inside the range [0,1]. Numerous parameters that needed to be optimized were represented by the search space. The boundaries [0,1] showed that during optimization, the system parameters were normalized within this range. The degree to which the alpha wolf affected the wolf positions was determined by the alpha coefficient. A rating of 0.5 indicated that the alpha wolf had a moderate influence. The greatest solution was the alpha wolf, and the other wolves' position updates were greatly impacted by its location. The best solution was given greater weight when the alpha value was higher, which sped up convergence at the expense of diversity. In addition, more exploration was promoted by a lower alpha value, with balance between exploration and exploitation was struck with the value of 0.5. The beta wolves have been the 2nd best with a value of 0.62. from this value it was shown that the alpha wolf was showed more impact than the 2nd options. The second solution which is the beta wolves helped the algorithm in determining a better global solution, when high value means of giving more weight that enhance the overall optimization process. The 3rd best solution was the delta wolves that was lower than alpha and beta but also contribute to search direction. The delta wolves appeared to have a moderate impact, as shown by the score of 0.57. They assisted in exploring and honing the search space, even though they weren't thought to be as dominating as the alpha and beta wolves. Like the beta value, a higher delta value led to more exploration of the search space, but a lower delta value accelerated convergence to the most

well-known solutions. After 200 iterations or if the goal function did not improve after a predetermined number of iterations, the optimization was terminated. The optimization process was kept from running too long and wasting computational resources because to the 200 iterations, which offered a clear end point. During these iterations, the optimization process was assessed to determine whether the algorithm was achieving the intended optimization targets maximizing PPV and minimizing overshoot and how well it was converging. Tables 1, 2 and Table 3 present the solutions with iteration numbers specification based on IGWO at no load, 2500 and 3000 conditions. Table 1 shows the performance under no-load conditions, where the power is generated by the system with zero connected load. The PL values reflect the generated power instead of the power consumed by a load. Also, the PV efficiency which is denoted as ηPV in Table 1 was calculated as the ratio of the PPV to the total input power available from the solar irradiation. Figures 9, 10 and Figure 11 show the Box and Whisker graph that related to the above parameters and constraints. In this work, it has to be noted that the PV irradiance was initialized at 1000 W/m² and moved into 2000 until it reached the maximum power of 6000 W. The tables from Table 1-3 showed the results of the IGWO-based MPPT controller under different cases of PL, ranging from very low load until the highest load. The PV power that denoted as (PPV) and efficiency of the PV grid denoted as (ηPV) were measured at each iteration of the IGWO optimization process.

Table 1. Solutions with iteration numbers based on IGWO at no-load conditions (PL=0W)

Iteration	P_L (W)	V_{DC}(V)	Overshoot in V_{DC} (V)	P_{PV} (W)	Overshoot in P_{PV} (W)	η_{PV}(%)
1	5800	370	80	5850	90	97.8
2	5900	369	78	5900	95	98.0
3	5700	372	85	5750	105	97.5
4	5950	373	90	5950	110	98.2
5	5900	370	77	5900	100	98.0
6	6000	374	95	6000	120	98.5
7	5800	369	76	5850	95	97.7
8	5900	371	78	5900	100	98.1
9	5950	370	80	5950	105	98.3
10	6000	374	85	6000	115	98.4
11	5850	369	77	5850	90	97.9
12	5900	371	75	5900	100	98.0
13	5700	372	80	5750	105	97.6
14	5950	373	88	5950	110	98.2
15	5900	371	79	5900	100	98.1
16	5900	371	75	5900	100	98.3
17	5800	370	82	5850	95	97.8
18	5950	373	85	5950	110	98.3
19	5900	371	78	5900	100	98.0
20	6000	375	90	6000	120	98.5

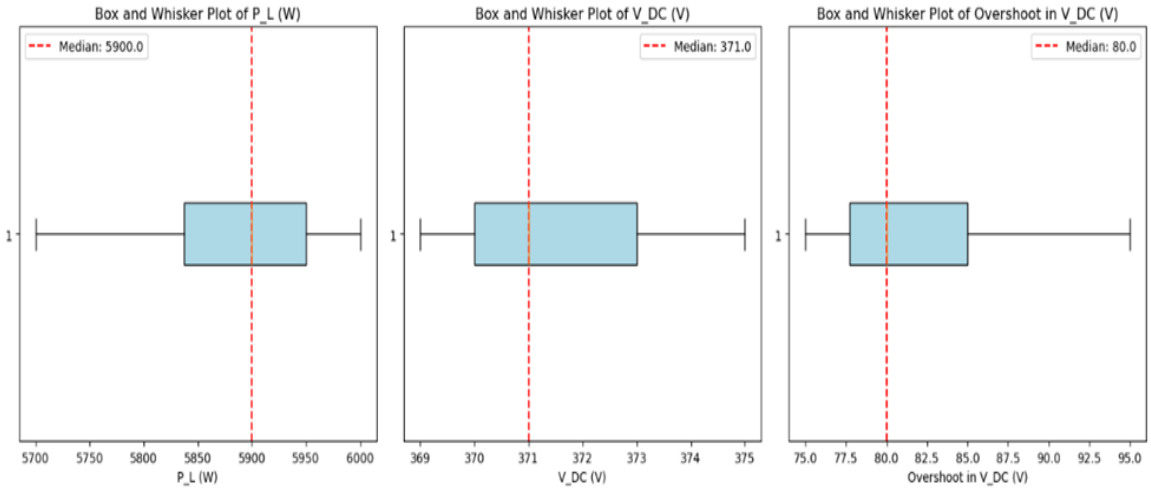

Figure 9. Box and Whisker graph based on IGWO at at no-load conditions (PL = 0 W)

Table 2. Solutions with iteration numbers based on IGWO at medium-load conditions (PL= 2000W)

Iteration	P_L (W)	V_{DC}(V)	Overshoot in V_{DC} (V)	P_{PV} (W)	Overshoot in P_{PV} (W)	η_{PV}(%)
1	5800	370	80	5850	90	97.8
2	5900	369	78	5900	95	98.0
3	5700	372	85	5750	105	97.5
4	5950	373	90	5950	110	98.2
5	5900	370	77	5900	100	98.0
6	6000	374	95	6000	120	98.5
7	5800	369	76	5850	95	97.7
8	5900	371	78	5900	100	98.1
9	5950	370	80	5950	105	98.3
10	6000	374	85	6000	115	98.4
11	5850	369	77	5850	90	97.9
12	5900	371	75	5900	100	98.0
13	5700	372	80	5750	105	97.6
14	5950	373	88	5950	110	98.2
15	5900	371	79	5900	100	98.1
16	5900	371	75	5900	100	98.3
17	5800	370	82	5850	95	97.8
18	5950	373	85	5950	110	98.3
19	5900	371	78	5900	100	98.0
20	6000	375	90	6000	120	98.5

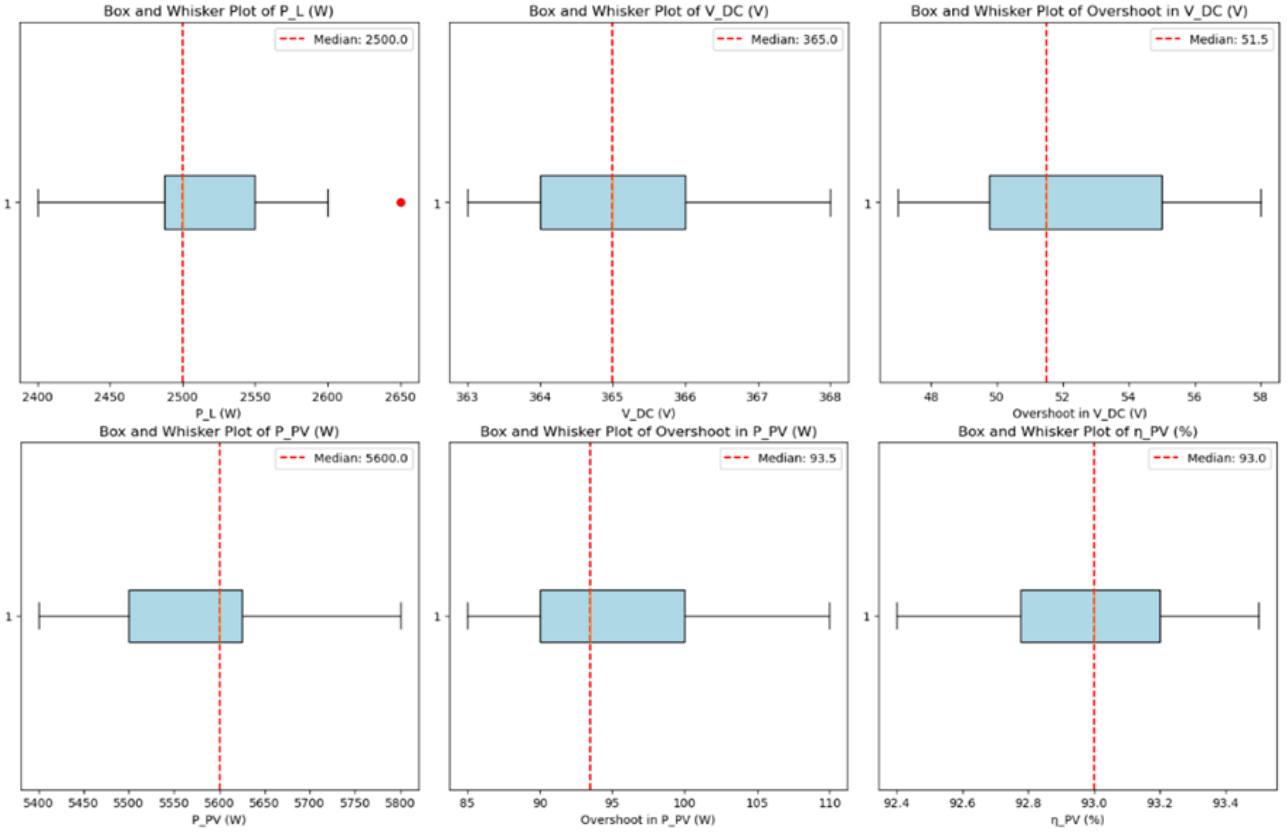

Figure 10. Box and Whisker graph based on IGWO at medium-load conditions (PL = 2000 W)

Table 3. Solutions with iteration numbers based on IGWO at high-load conditions (PL= 3000W)

Iteration	P_L (W)	V_{DC}(V)	Overshoot in V_{DC} (V)	P_{PV} (W)	Overshoot in P_{PV} (W)	η_{PV}(%)
1	2900	368	38	5850	100	97.8
2	3000	369	37	5890	105	98.0
3	3100	370	40	5950	110	98.2
4	2800	367	42	5750	98	97.7

5	2900	368	39	5850	101	97.9
6	3000	369	36	5890	104	98.0
7	3100	370	41	5950	110	98.3
8	2800	367	43	5750	97	97.6
9	3000	369	38	5890	102	98.0
10	2900	368	39	5850	99	97.9
11	3100	370	40	5950	106	98.2
12	2800	367	41	5750	95	97.6
13	3000	369	36	5890	103	98.0
14	3000	369	36	5890	104	98.1
15	2900	368	38	5850	100	97.8
16	3100	370	42	5950	110	98.3
17	2800	367	44	5750	96	97.7
18	2900	368	40	5850	98	97.9
19	3000	369	37	5890	105	98.0
20	3100	370	43	5950	111	98.4

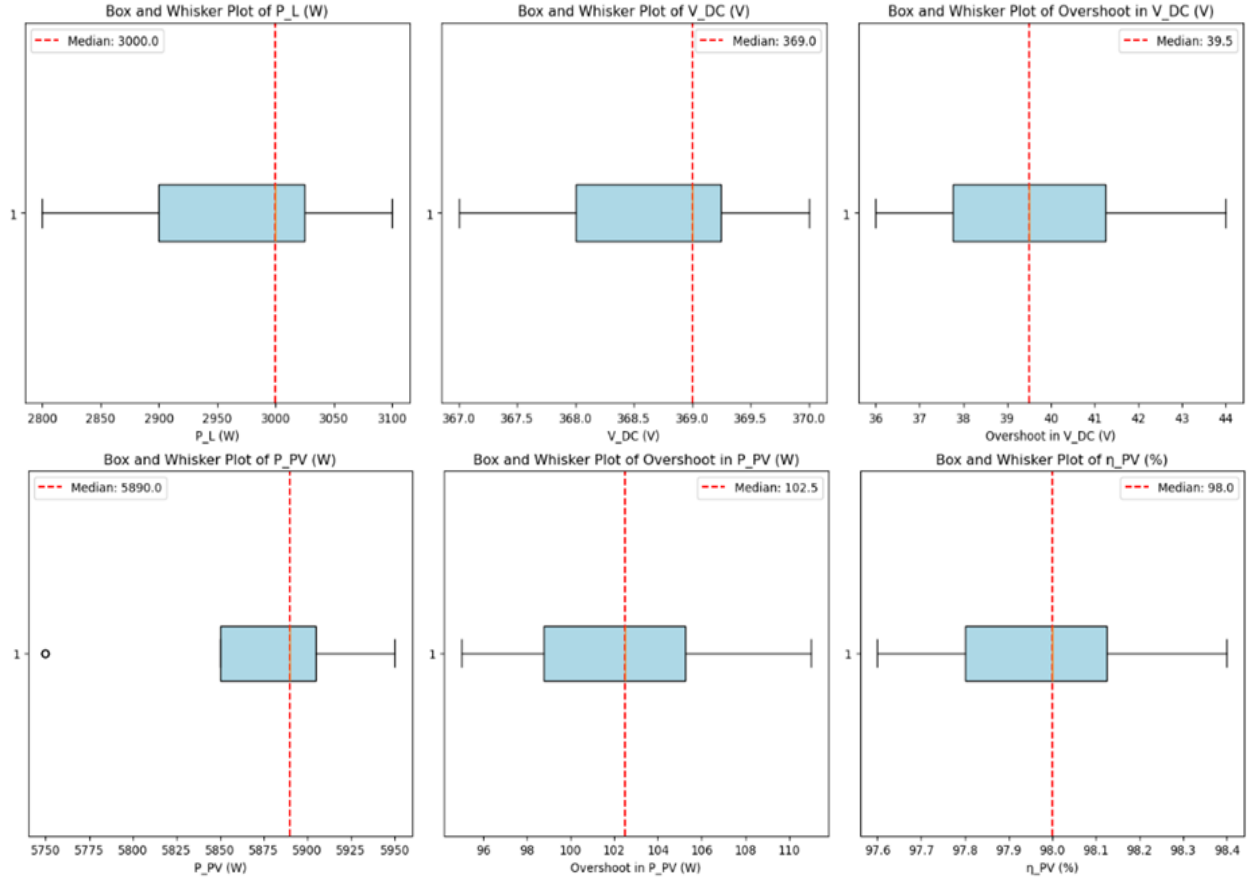

Figure 11. Box and Whisker graph based on IGWO at high-load conditions (PL= 3000W)

3.2 Test performance under fast change in load

Within the framework of the suggested EMS, the grid-tied inverter's performance was assessed in this part using two distinct MPPT control techniques: the optimized MPPT control and the conventional classical MPPT. The MATLAB Simulink software was used to run the simulations. The PV system's and the battery's DC/DC converters were used to control the power switches' respective control functions. The DC/AC inverter was set up for single-phase operation and is controlled by PWM using the dq control method. A temperature of 25°C and a solar irradiation of 1000 W/m² were used for the simulation, which produced 6000 W of solar power. The AC bus on the inverter side was used to connect a nonlinear load to the grid. Table 4 contains the grid specifications that were employed in this study, while Table 5 lists the parameters for the solar array and batteries. In this section, it had to be noted that the test measurements were under several load changes as mentioned through Tables 1-3, while varying the load power dynamically to evaluate the IGWO-based MPPT controller's response.

Table 4. Main grid specifications

Parameter	Value
Grid voltage	66 kV
DC bus voltage	375 V
Grid frequency	60 Hz
PWM frequency	10kHz
Inverter voltage (RMS bus voltage)	230 V

To illustrate the dynamic response of the inverter and the suggested EMS under the IGWO-based MPPT control, a 3-second simulation is run in this section. By optimizing the PV system's power production, this strategy improves system performance. Consequently, the technique lowers the PV array's steady-state power oscillations, improving overall performance. Figure 12 provides a graphic representation of this improvement.

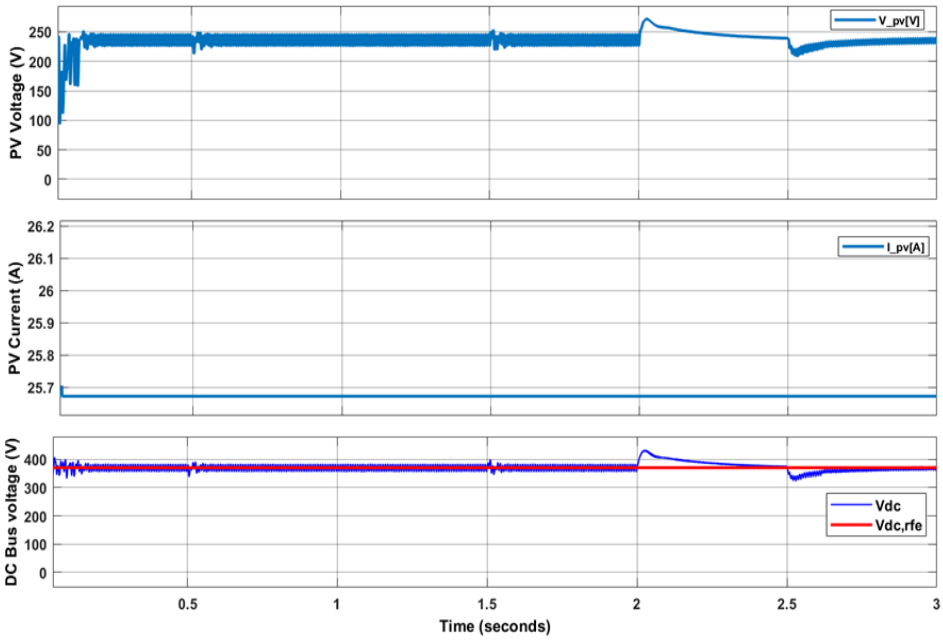

Figure 12. PV results under IGWO based MPPT

With very slight variations in the power curve, especially around t = 2 seconds, the MPP varies in accordance with changes in the load. The system maintains steady operation during this time by adapting to changes in load. Furthermore, between t = 2 and t = 3 seconds, the battery switches to discharge mode. The grid is not linked to the inverter during this time, and the battery provides the load with positive output power. As a result, the solar array and batteries cooperate to meet the load demand. The grid results and inverter voltage and current curves during this operation are shown in Figures 13 and 14, which also illustrates how the inverter behaves when the grid is cut off and the load is supplied by the battery and solar array. These values are adapted from parameters used in prior studies such in [1, 6], to ensure consistency with widely accepted modeling practices and to reflect a realistic mid-scale PV-battery configuration.

The values for the inductor and capacitor used in the DC-DC boost converter as given in Table 5 were determined based on standard design procedures. Below is the equation used for selecting these the inductor as in equation below:

$$L = V_{in} \cdot \frac{V_{out} - V_{in}}{f_s \cdot \Delta I_L \cdot V_{OUT}} \quad (15)$$

Where V_{in}=200 V, V_{out}=375 V, f_s=10 kHz, ΔI_L=20% of peak load current which was assumed to be 25A that given inductor value of 1mH. While, the output capacitor is selected to reduce the voltage ripple on the output side and estimated using the following equation:

$$C = I_{load} \cdot D \cdot \frac{1-D}{f_s \cdot \Delta V_{out}} \quad (16)$$

where I_{load}=25 A and ΔV_{out}=1 that given the capacitor value of 2000μF.

The control strategy for voltage regulation in the proposed system relies on the DC-AC inverter's operation using PWM and a dq control method to ensure frequency synchronization with the grid normal operation. Under grid-connected conditions, the inverter continuously adjusts to match the grid voltage. When the grid is disconnected at t=2sec, the system transitions to disconnected mode, and the battery provided power to the load. During this transition, the inverter switches to supplying power autonomously without grid support. The inverter output voltage was regulated based on DC voltage and the requirements regarding the load changes. Also, the transition between connected and disconnected operation, resulting higher output voltage. In grid-connected mode, the inverter synchronizes with the grid voltage and frequency. However, when the grid disconnects, the inverter relies on its internal control mechanisms to generate a stable AC output for the load. This results in an initial voltage

fluctuation as the inverter adjusts to the new operating conditions and the battery begins to supply the load.
This voltage increase can be affected by the lack of grid impedance, which provided a stabilizing effect on voltage in grid-connected systems. Once the grid is disconnected, the inverter operates without this impedance, which lead to a brief overshoot in the output voltage. The voltage regulation in disconnecting mode is also influenced by the battery control and the EMS, which adjusts the output to ensure stable operation.

Parameter	Value
Maximum power of PV system	6000 W
Maximum PV voltage	240V
Maximum PV current	25 A
Switching frequency	10kHz
Boost converter inductance	1mH
Boost converter output capacitance	2000 uF
Battery voltage	200 V
Rated capacity	40 Ah
Initial SOC	80 %

Table 5. Main grid specifications

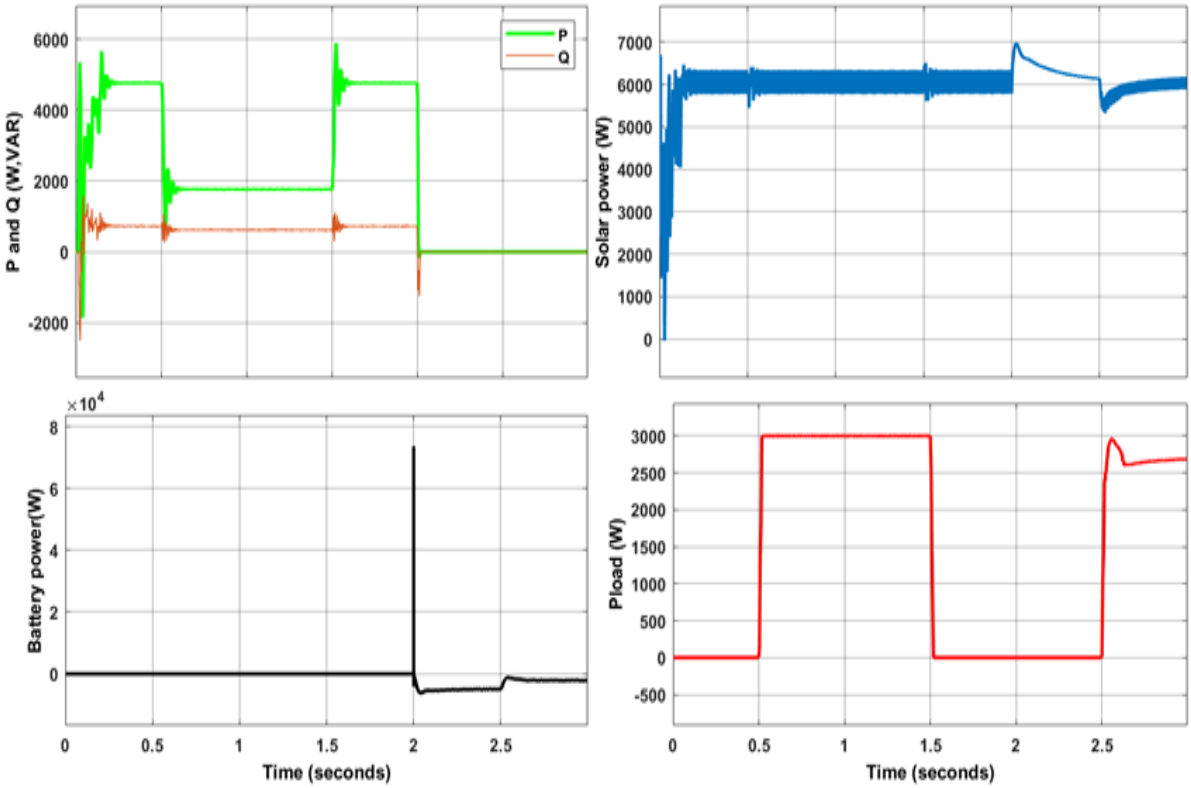

Figure 13. power curves for grid, battery, solar system and load.

3.3 Comparison with state-of-arts methods

3.3.1 The main Results

When compared to conventional techniques, the suggested system exhibits better stability in terms of oscillations, speed, and accuracy. Compared to traditional methods, the novel optimization-based MPPT approach has several advantages. As shown in Figure 14, it increases energy efficiency, better adjusts to changing climatic circumstances, and may be used with a variety of PV systems. The suggested IGWO approach improves accuracy, lowers expenses, and offers fault detection capabilities, as the figure illustrates. The suggested approach shows excellent efficiency in capturing peak power and maintains MPP tracking under various load scenarios. The system achieves a peak power output of 5900 W with a maximum efficiency of 98.3%. This results proved the tracking performance and is near the theoretical peak power of 6000 W. The traditional P&O approach only produces 5400 W of electricity and has a lower efficiency of 90%. Additionally, the suggested approach provided quick convergence speed, and efficient DC bus voltage regulation as shown in Figure 15.

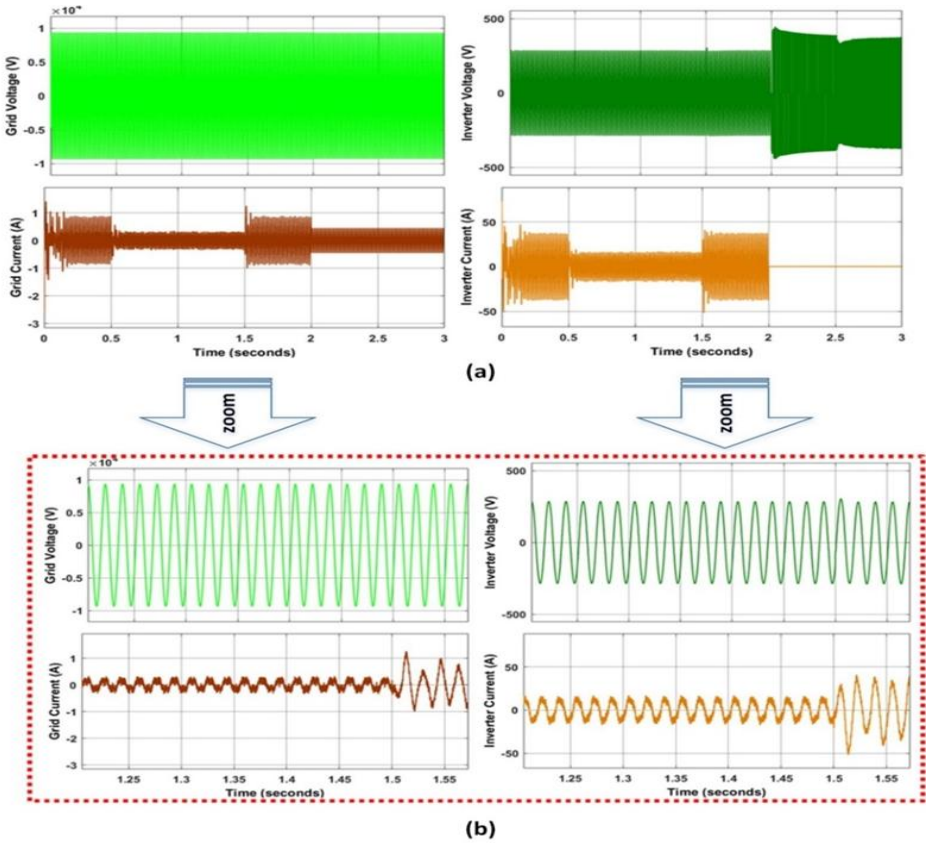

Figure 14. (a) Grid and inverter results under IGWO control (b) sample zoom of the results

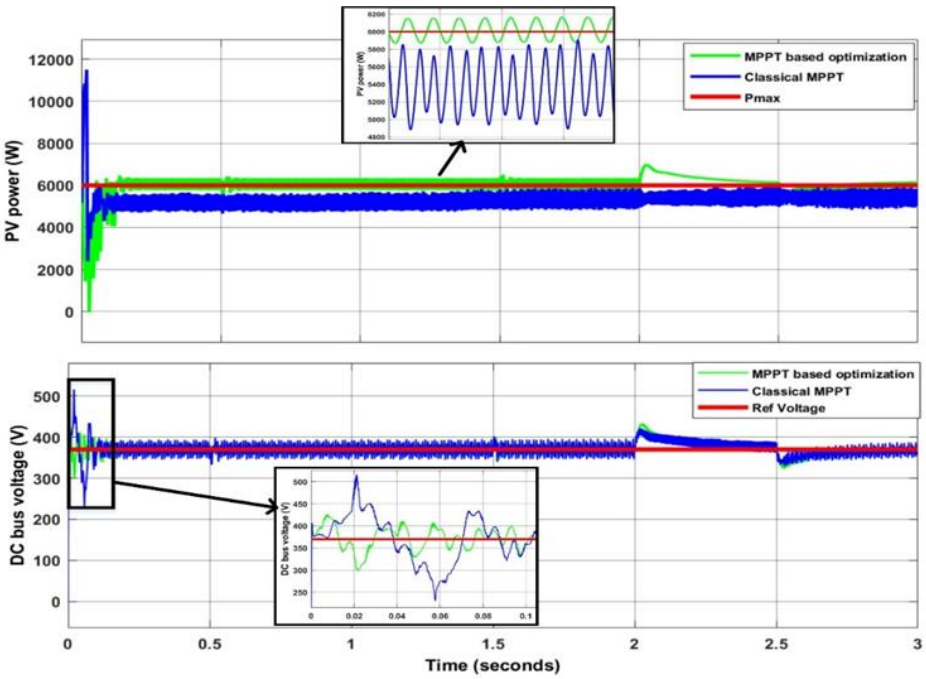

Figure15. Performance comparison of IGWO-based MPPT and classical P&O method

A comparison between the proposed control technique and the traditional P&O method with dq inverter control is done in order to illustrate the efficacy of the suggested method. Table 6 presented a comparison of the two approaches based on PL and grid condition. A comparison of each algorithm's DC bus voltage and overshoot is also included. The average voltage levels for both the IGWO and dq approaches are greater than those for the P&O and dq control. This have been indicating that the suggested method produced a more stable DC bus voltage. Also, the PV power generated by the suggested method was higher than that of the traditional way. The traditional P&O approach only produces 5400 W, but the suggested way provided 5900 W. The suggested approach produces a very high-power output considering the theoretical maximum power of

6000 W. In comparison to the conventional method, the suggested method exhibits greater efficiency, with a maximum efficiency of 98.3%. Additionally, the suggested technique greatly lessens the PV system's power oscillations. While the P&O approach sees far bigger oscillations, up to 800 W, the oscillation around the Maximum Power Point (MPP) is limited to just 88 W. Because of this, the IGWO method has a very low power loss, which makes it an extremely effective strategy for maximum power tracking. The performance of the conventional P&O approach and the suggested IGWO-based MPPT method under various load situations is contrasted in Table 6. DC bus voltage (VDC), overshoot in VDC, PV power output (PPV), overshoot in PV power, and overall efficiency (ηPV) are among the important parameters it assesses. The first finding is that, at all load levels, the IGWO approach consistently produces a greater DC bus voltage (VDC) than the P&O method. For example, P&O only reaches 366 V when there is no load, whereas IGWO hits 371 V. The IGWO technique maintains somewhat higher voltage levels with larger loads, such as 365 V as opposed to 360 V at a 2500 W load, continuing this trend. Better voltage regulation, which is necessary for system stability and ideal power conversion, is suggested by the higher voltage levels in the IGWO approach. The variation in overshoot levels for the DC bus voltage is another significant discovery. Under all load circumstances, the IGWO approach exhibits noticeably less voltage overshoot than the P&O method. For instance, IGWO has a 75 V voltage overrun at no load, while P&O has a substantially greater overshoot of 125 V. With voltage overshoots of 47 V and 36 V, respectively, at 2500 W and 3000 W loads, the IGWO technique continues to outperform P&O, which has overshoots of 103 V and 110 V. This decreased overshoot suggests that the IGWO technique offers more consistent voltage management, lowering the possibility of high voltage spikes causing component stress or damage. The IGWO technique continuously produces more PV power than the P&O approach in terms of power production. For instance, the P&O approach only produces 5400 W with no load, whereas the IGWO method produces 5900 W. In a similar vein, IGWO produces greater power outputs (e.g., 5600 W and 5890 W) at 2500 W and 3000 W loads than the P&O approach (e.g., 5200 W and 5440 W). These findings suggest that, particularly when load circumstances vary, the IGWO approach is more successful in obtaining the most power possible from the photovoltaic system. Furthermore, the IGWO approach has a noticeably less overrun in PV power output. In contrast to P&O, which has a much larger power overrun of 800 W at no load, IGWO only has 100 W. In a similar vein, IGWO exhibits less power fluctuation at higher loads, with overshoots of 88 W at 2500 W and 104 W at 3000 W, but P&O has much larger overshoots. This reduced power overshoot illustrates how the IGWO technique can sustain more reliable and effective power extraction, reducing energy losses brought on by variations in power output. Lastly, compared to the P&O method, the suggested IGWO method has a significantly higher efficiency. At no load, IGWO's efficiency is 98.3%, while P&O's is only 90%. P&O's efficiencies are lower at 86.6% and 90.6%, while IGWO maintains efficiencies of 93.3% and 98.1% for 2500 W and 3000 W loads, respectively. The IGWO method's increased efficiency highlights its greater capacity to identify the maximum power point and transform it into usable energy, which leads to a more efficient solar system. The suggested IGWO-based MPPT approach performs better than the traditional P&O approach in every assessed metric, such as overall efficiency, power overshoot control, PV power output, and DC bus voltage stability. Because of these benefits, the IGWO approach is a more dependable and effective way to maximize energy output from photovoltaic systems, especially when load conditions are dynamic or changeable.

Table 6. Output power and efficiency comparison between IGWO-based MPPT and classical MPPT

P_L (W)	MPPT method	V_{DC}(V)	Overshoot in V_{DC} (V)	P_{PV} (W)	Overshoot in P_{PV} (W)	η_{PV}(%)
1000	P&O	366	125	5400	800	90
1000	IGWO	371	75	5900	100	98.3
2500	P&O	360	103	5200	700	86.6
2500	IGWO	365	47	5600	88	93.3
3000	P&O	362	110	5440	650	90.6
3000	IGWO	369	36	5890	104	98.1

3.3.2 Impact of IGWO on Grid-Side Performance

As the obtained results the grid-side inverter employs a good dq control strategy in both cases. The proposed IGWO-based MPPT improved the quality of power injected into the grid by minimizing the PV power oscillations and DC-link voltage ripple. That was mean, the IGWO algorithm provided a more stable input to the inverter, referring to improve current controller performance. As shown in Figure 16, the DC-link voltage ripple has been reduced from 15 V under the

P&O-based MPPT to about 4V with the proposed IGWO-based MPPT. This minimization directly contributed to improved grid current quality, as confirmed by the FFT analysis in Figure 16. In the other hand, Table 7 showed a notable reduction in the THD, improved power factor, and enhanced voltage/frequency regulation. These results demonstrated that, while IGWO is not directly applied to the inverter control, its indirect coupling through DC-link stabilization enables a unified control framework that enhances overall grid performance. Figure 17 showed the FFT analysis of grid current under the traditional and the proposed model. The IGWO-based provided high reduction in THD as confirmed in Table7.

Table 7. Grid-side performance comparison under identical dq control

Metric	P&O–MPPT + dq	IGWO–MPPT + dq
Grid RMS voltage deviation (%)	±1.8	±0.6
Frequency deviation (Hz)	±0.15	±0.04
Grid current THD (%)	4.9	2.1
Power factor	0.96	0.995

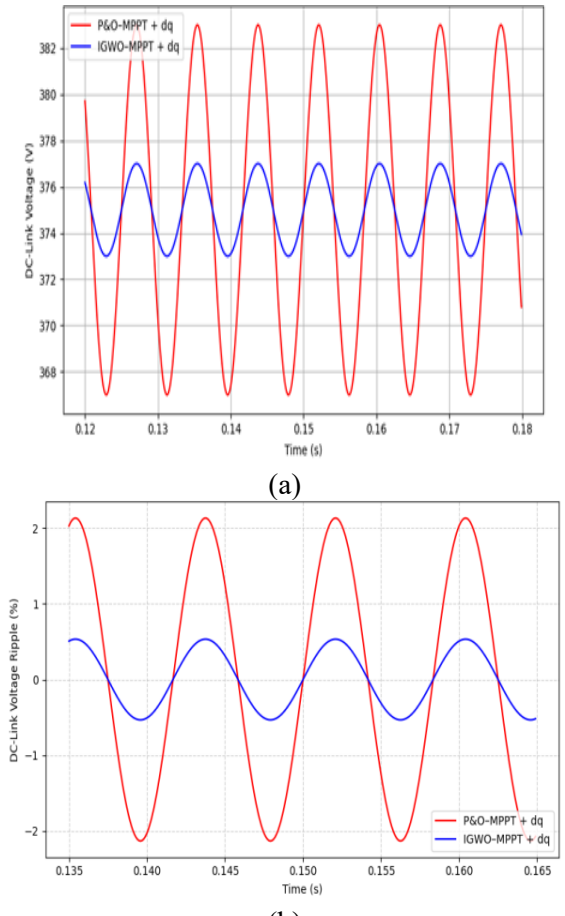

Figure 16. Grid-Side Performance Comparison for (a) DC-link voltage ripple normalized to percentage of nominal voltage and (b) DC-link voltage ripple in volts (absolute voltage values)

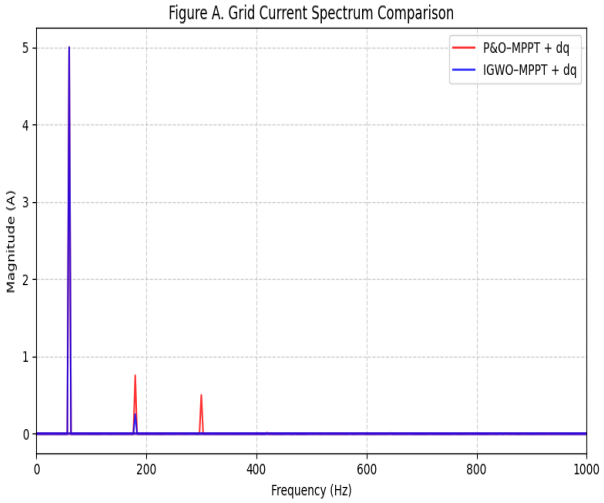

Figure 17. Grid current harmonic spectrum under P&O–MPPT and IGWO–MPPT

4. CONCLUSIONS

This study proposed an optimization-based control strategy for a battery-integrated photovoltaic (PV) system operating within a microgrid (MG) environment. By applying the Improved Grey Wolf Optimizer (IGWO) to enhance the Maximum Power Point Tracking (MPPT) process, the system achieved superior dynamic response, reduced power oscillations, and improved energy conversion efficiency compared to the conventional Perturb and Observe (P&O) method. The simulation results demonstrated that the IGWO-based MPPT algorithm consistently delivered higher DC voltage and photovoltaic power (PPV) under varying load conditions. For instance, under no-load conditions, the IGWO achieved 371 V compared to 366 V from the P&O method, and 5900 W of PPV compared to 5400 W. Additionally, the IGWO algorithm showed significantly reduced overload behaviour which is an important indicator of control stability with a voltage overshoot of only 75 V, in contrast to 125 V for P&O. These findings underline the effectiveness of the proposed approach in maintaining power quality and system reliability. However, while the IGWO technique shows promise in simulation, its real-world deployment on large-scale PV systems have practical challenges such as computational complexity and integration with existing smart inverter technologies. Newer research should explore real-time hardware implementation and consider hybrid optimization strategies to further enhance adaptability and resilience under diverse operating conditions. In conclusion, the IGWO-based MPPT controller provides a viable pathway for improving energy efficiency and operational stability in grid-connected PV systems. Its lies in optimizing not just energy extraction but also maintaining grid voltage and frequency within acceptable limits critical factors for modern, intelligent power networks.

REFERENCES

[1] N. Mendis, M. A. Mahmud, T. K. Roy, M. E. Haque, and K. M. Muttaqi, "Power management and control strategies for efficient operation of a solar power dominated hybrid DC microgrid for remote power applications," 2016, doi: 10.1109/IAS.2016.7731816.

[2] M. Singh, L. A. C. Lopes, and N. A. Ninad, "Grid forming Battery Energy Storage System (BESS) for a highly unbalanced hybrid mini-grid," Electr. Power Syst. Res., vol. 127, 2015, doi: 10.1016/j.epsr.2015.05.013.

[3] I. K. Amin, M. N. Uddin, and J. A. Cotter, "A PV-coupled Battery Energy Storage System Incorporated with PSO-ANFIS based MPPT Controller for Standalone Mode," in Conference Record - IAS Annual Meeting (IEEE Industry Applications Society), 2021, vol. 2021-October, doi: 10.1109/IAS48185.2021.9677169.

[4] A. Pradipta, D. C. Riawan, and Soedibyo, "Power flow control of battery energy storage system using droop voltage regulation technique integrated with hybrid PV/Wind generation system," in 2018 International Conference on Information and Communications Technology, ICOIACT 2018, 2018, vol. 2018-January, doi: 10.1109/ICOIACT.2018.8350704.

[5] M. Patel and S. Bohra, "Power management of grid-connected PV wind hybrid system incorporated with energy storage system," Futur. Energy, vol. 2, no. 3, 2023, doi: 10.55670/fpll.fuen.2.3.2.

[6] A. Mahesh, K. S. Sandhu, and J. V. Rao, "Optimal Sizing of Battery Energy Storage System for Smoothing Power Fluctuations of a PV/Wind Hybrid System," Int. J. Emerg. Electr. Power Syst., vol. 18, no. 1, 2017, doi: 10.1515/ijeeps-2016-0105.

[7] I. Masenge and F. Mwasilu, "Hybrid Solar PV-Wind Generation System Coordination Control and Optimization of Battery Energy Storage System for Rural Electrification," 2020, doi: 10.1109/PowerAfrica49420.2020.9219890.

[8] M. Z. Daud, A. Mohamed, M. Z. Che Wanik, and M. A. Hannan, "Performance evaluation of grid-connected photovoltaic system with battery energy storage," 2012, doi: 10.1109/PECon.2012.6450234.

[9] P. Verma, P. Mahajan, and R. Garg, "DC Link Voltage Control of Stand-Alone PV Tied with Battery Energy Storage System," 2021.

[10] B. Jena, S. Goel, and R. Sharma, "Smoothing control scheme of photovoltaic module through a battery energy storage system," Int. J. Eng. Adv. Technol., vol. 8, no. 6 Special Issue 3, 2019, doi: 10.35940/ijeat.F1308.0986S319.

[11] J. Li, Y. Qiao, G. Liu, and Z. Lu, "Capacity Configuration of Battery Energy Storage System for Photovoltaic Generation System Considering the High Chargerate," in E3S Web of Conferences, 2020, vol. 182, doi: 10.1051/e3sconf/202018203003.

[12] X. Hai, L. Yin, Z. Jia, Q. Yu, Y. Wang, and D. Yao, "Optimizing capacity configuration of photovoltaic and battery energy storage systems in EV charging station based on time-of-use pricing," in IOP Conference Series: Materials Science and Engineering, 2019, vol. 486, no. 1, doi: 10.1088/1757-899X/486/1/012062.

[13] W. Xiong, J. Zeng, L. Wu, and H. Cheng, "Power management of a residential hybrid photovoltaic inverter with battery energy storage system," 2019, doi: 10.1109/PEDG.2019.8807638.

[14] A. Subramanian and J. Raman, "Grasshopper optimization algorithm tuned maximum power point tracking for solar photovoltaic systems," J. Ambient Intell. Humaniz. Comput., vol. 12, no. 9, 2021, doi: 10.1007/s12652-020-02593-9.

[15] M. A. Khazain, N. M. Hidayat, K. Burhanudin, and E. Abdullah, "Boost Converter of Maximum Power Point Tracking (MPPT) Using Particle Swarm Optimization (PSO) Method," 2021, doi: 10.1109/ICSGRC53186.2021.9515228.

[16] N. Cao and J. Liu, "An improved maximum power point tracking for photovoltaic grid-connected inverter," 2013, doi: 10.1109/ICMA.2013.6617987.

[17] S. V. Dhople, A. Davoudi, G. Nilles, and P. L. Chapman, "Maximum power point tracking feasibility in photovoltaic energy-conversion systems," 2010, doi: 10.1109/APEC.2010.5433556.

[18] Selvam R, "Design and Implementation of an Intelligent Maximum Power Point Tracking Controller for Dual-Axis Solar Tracking Photovoltaic Systems," INTERANTIONAL J. Sci. Res. Eng. Manag., vol. 08, no. 05, 2024, doi: 10.55041/ijsrem33623.

[19] U. U. Rehman, P. Faria, L. Gomes, and Z. Vale, "Artificial Neural Network Based Efficient Maximum Power Point Tracking for Photovoltaic Systems," 2022, doi: 10.1109/EEEIC/ICPSEurope54979.2022.9854613.

[20] K. Ullah, M. Ishaq, F. Tchier, H. Ahmad, and Z. Ahmad, "Fuzzy-based maximum power point tracking (MPPT) control system for photovoltaic power generation system," Results Eng., vol. 20, 2023, doi: 10.1016/j.rineng.2023.101466.

[21] M. S. Mohammed, A. H. Saleh, H. K. AL-Qaysi, and R. A. Vural, "Finite automated system to design a high efficiency LLC resonant converter system for 3 kW. PV solar array," e-Prime - Adv. Electr. Eng. Electron. Energy, vol. 10, 2024, doi: 10.1016/j.prime.2024.100770.

[22] M. S. Mohammed and R. A. Vural, "Evolutionary Design Automation of High Efficiency Series Resonant Converter for Photovoltaic Systems," IEEE Trans. Power Electron., vol. 35, no. 11, 2020, doi: 10.1109/TPEL.2020.2987086.

[23] [23] R. M. Imran and K. H. Chalok, "Innovative mode selective control and parameterization for charging Li-ion batteries in a PV system," AIMS Energy, vol. 12, no. 4, 2024, doi: 10.3934/energy.2024039.

[24] M. S. Mohammed and R. Acar Vural, "A High Efficiency Design of PV-Array Dimension Optimization for Shaded and Non-Shaded Configuration," 2019, doi: 10.1109/GCAT47503.2019.8978349.

[25] I. S. Millah, P. C. Chang, D. F. Teshome, R. K. Subroto, K. L. Lian, and J. F. Lin, "An Enhanced Grey Wolf Optimization Algorithm for Photovoltaic Maximum Power Point Tracking Control Under Partial Shading Conditions," IEEE Open J. Ind. Electron. Soc., vol. 3, 2022, doi: 10.1109/OJIES.2022.3179284.

[26] H. Alhumade, H. Rezk, M. Louzazni, I. A. Moujdin, and S. Al-Shahrani, "Advanced Energy Management Strategy of Photovoltaic/PEMFC/Lithium-Ion Batteries/Supercapacitors Hybrid Renewable Power System Using White Shark Optimizer," Sensors, vol. 23, no. 3, 2023, doi: 10.3390/s23031534.

[27] S. J. Yaqoob, S. Motahhir, and E. B. Agyekum, "A new model for a photovoltaic panel using Proteus software tool under arbitrary environmental conditions," J. Clean. Prod., vol. 333, 2022, doi: 10.1016/j.jclepro.2021.130074.

[28] S. J. Yaqoob, A. L. Saleh, S. Motahhir, E. B. Agyekum, A. Nayyar, and B. Qureshi, "Comparative study with practical validation of photovoltaic monocrystalline module for single and double diode models," Sci. Rep., vol. 11, no. 1, 2021, doi: 10.1038/s41598-021-98593-6.

[29] A. S. Shaeel, H. H. Abed, and A. F. Al-Baghdadi, "Modeling and Detection of Cyber and Physical Attacks on the Control Unit of PV Farm System," Diyala J. Eng. Sci., vol. 18, no. 2, 2025, doi: 10.24237/djes.2025.18210.

[30] W. Chen, W. T. Chen, M. Saif, M. F. Li, and H. Wu, "Simultaneous Fault Isolation and Estimation of Lithium-Ion Batteries via Synthesized Design of Luenberger and Learning Observers," IEEE Trans. Control Syst. Technol., vol. 22, no. 1, 2014, doi: 10.1109/TCST.2013.2239296.

[31] S. J. Yaqoob, J. K. Raham, and H. A. Sadiq, "Analysis and Simulation of Current-source Flyback Inverter with Efficient

BCM Control Strategy," WSEAS Trans. Electron., vol. 12, 2021, doi: 10.37394/232017.2021.12.18.

[32] A. L. Saleh, A. A. Obed, Z. A. Hassoun, and S. J. Yaqoob, "Modeling and Simulation of A Low Cost Perturb& Observe and Incremental Conductance MPPT Techniques in Proteus Software Based on Flyback Converter," in IOP Conference Series: Materials Science and Engineering, 2020, vol. 881, no. 1, doi: 10.1088/1757-899X/881/1/012152.

[33] S. Mirjalili, S. Mohammad, and A. Lewis, "Advances in Engineering Software Grey Wolf Optimizer," Adv. Eng. Softw., vol. 69, 2014.

[34] S. N. Makhadmeh et al., "Recent Advances in Grey Wolf Optimizer, its Versions and Applications: Review," IEEE Access, vol. 12, 2024, doi: 10.1109/ACCESS.2023.3304889.

[35] A. M. Eltamaly and Z. A. Almutairi, "A novel star-nosed mole optimization algorithm applied for MPPT of PV systems," Sci. Rep., vol. 15, no. 1, 2025, doi: 10.1038/s41598-025-02938-4.